North Atlantic sea level budget revisited

Zhe Song[1,2], Anny Cazenave[1], William Llovel[2], Andrea Storto[3] and Marie Bouih[4]

[1]Université de Toulouse, LEGOS (CNES/CNRS/IRD/UT3), 31401 Toulouse, CEDEX 9, France
[2]Université de Bretagne Occidentale, CNRS, Ifremer, IRD, Laboratoire d'Océanographie Physique et Spatiale (LOPS), IUEM, 29280, Plouzané, France
[3]Institute of Marine Science, National Research Council of Italy, Rome, Italy
[4]Magellium, 31520 Ramonville St Agne, France

Corresponding authors: Zhe Song (zhe.song@univ-brest.fr) and Anny Cazenave (anny.cazenave@univ-tlse3.fr, anny.cazenave@gmail.com)

Ocean Science

3rd revised version

14 September 2026

Abstract

Based on satellite altimetry, GRACE space gravimetry and Argo-based steric data down to 2000m, recent studies have shown that the North Atlantic sea level budget (i.e., altimetry-based sea level minus sum of components) of the past two decades is not closed, with strong regional residuals in the North Atlantic. In this study, we revisit the North Atlantic sea level budget, using satellite altimetry, GRACE and GRACE-FO data, different Argo products and an ocean reanalysis (CIGAR) over the 2004-2022 time span. The ocean reanalysis is used to estimate the manometric contribution, an alternative to using GRACE data, as well as the deep ocean contribution to the sea level budget, not yet fully sampled by Argo. Analyzing different data sets allows us to assess their impact on the previously reported non-closure of the North Atlantic sea level budget. We first find that using the CIGAR ocean reanalysis-based manometric component significantly reduces the residuals of the North Atlantic sea level budget compared to GRACE. We also find that accounting for the deep ocean (below 2000m) thermal expansion (using the CIGAR reanalysis) allows for reducing 30% the North Atlantic budget residuals when using both GRACE and CIGAR for the manometric component. The budget can be closed within the data uncertainties when CIGAR manometric and full depth steric sea level are included.

1 Introduction

While many studies have been devoted to assessing the global mean sea level budget over the satellite altimetry era (1993 to present) (e.g., Barnoud et al., 2021; Bouih et al., 2025; Chen et al., 2020; Dieng et al., 2017; Horwath et al., 2022; Llovel et al., 2023; Nerem et al., 2018; WCRP, 2018), only a few have focused on the regional sea level budget, with mixed results (e.g., Bouih et al., 2025; Camargo et al., 2023; Frederikse et al., 2016; Hamlington et al., 2020; Mu et al., 2024; Royston et al., 2020). At the global scale, the two main contributors to the global mean sea level rise are ocean mass and thermosteric change. At regional scale, however, other factors play a non-negligible role, such as the halosteric (i.e., salinity-related) component, which makes the regional sea level budget more complex to assess. Considering all ocean basins, a recent study (Bouih et al., 2025) investigated the regional sea level trend budget closure over the 2004-2022 time span, using altimetry-based sea level data, GRACE space gravimetry for the regional ocean mass variations (also called manometric component, Gregory et al., 2019) and Argo data for the steric (sum of thermosteric and halosteric terms) component down to 2000 m (global mean trends removed from all data sets). Bouih et al. (2025) also considered several ocean reanalyses to compute the manometric component (an alternative to using GRACE data), following the approach developed by Camargo et al. (2023), i.e., using the sterodynamic sea level (Gregory et al., 2019) computed by the reanalysis and correcting it for the local steric effect. The Bouih et al. (2025)'s study used the Argo-based product from SIO (SCRIPPS Institution of Oceanography) that corrected for the spurious salinity drift reported recently in some Argo-based salinity measurements (Liu et al., 2020; Ponte et al., 2021; Wong et al., 2023). They showed that in the Pacific, Indian and South Atlantic oceans, the sea level budget trend residuals (altimetry-based sea level minus sum of components) were non-significant, considering the data uncertainties. On the other hand, strong positive residuals were observed in the North Atlantic, whatever the manometric component considered (i.e., either from GRACE or from ocean reanalyses).

In the present study we revisit the question of the North Atlantic sea level budget over the 2004-2022 time span, using a variety of different data sets for the components of the sea level budget: different GRACE mascon solutions and different Argo-based gridded products down to 2000m, as well as an ocean reanalysis that provide an estimate of the steric signal from the deep ocean. Our objective is to evaluate the impact of each product on the currently reported non-closure of the North Atlantic sea level budget. An important addition, compared to the Bouih et al. (2025)'s study, consists of accounting for the deep ocean warming below 2000m (not sampled by Argo) using estimates from the ocean reanalysis. This paper is organized as follows. Section 2 presents the data and analysis method. Section 3 displays the results for the North Atlantic sea level budget, both in terms of trend maps and time series. A synthesis of the results is presented in the Discussion section (section 4) with some highlights on the few main messages arising from this study.

2 Data and methods

2.1 Data

2.1.1 Altimetry-based total sea level

Sea level variations have been continuously measured by satellite altimetry since 1993. In this study, we use the daily 0.25° ×0.25° gridded sea level anomaly data, version DT2021 available from the Copernicus Climate Change Service (C3S) (Copernicus Climate Change Service, Climate Data Store, 2018; Accessed on 15-11-2025).
The data set is further corrected for the TOPEX-A instrumental drift that affected the first 6 years of the time series (Ablain et al., 2017), but the correction has no impact on our assessment that starts in 2004. The Jason-3 radiometer drift that impacts the wet troposphere correction (Brown et al., 2023) is corrected for. The altimetry data set is also corrected for the absolute Glacial Isostatic adjustment (GIA) effect, using the ICE6G-D model from Peltier et al. (2018).

2.1.2 GRACE-based ocean mass

The Gravity Recovery and Climate Experiment (GRACE) and GRACE Follow-On (GRACE-FO) are joint missions by the National Aeronautics and Space Administration (NASA) and the German Aerospace Center (DLR) (Tapley et al., 2019). These satellites have been measuring temporal variations in Earth's gravity field since 2002. This data set is essential for estimating mass redistribution in the oceans, terrestrial water storage, ice sheets, and glaciers. GRACE/GRACE-FO data are generally available in two forms: Spherical Harmonic (SH) coefficients and Mass Concentration (mascon) solutions. In Bouih et al. (2025), we used, in addition to the mascon solutions, an ensemble of 60 SH solutions (update of Blazquez et al. 2018). The sea level budget residuals based on this ensemble mean SH solution showed a strong north–south signal in the mid-North Atlantic, due to north–south stripe noise affecting SH solutions (see Blazquez et al. 2018 for a discussion). For that reason, we focus here on the mascon solutions. In this study, we utilize the latest Release 6 (RL06) mascon solutions provided by three different institutions: the Center for Space Research (CSR, Save et al., 2016), the Jet Propulsion Laboratory (JPL, Watkins et al., 2015), and the Goddard Space Flight Center (GSFC, Loomis et al., 2019b).

These mascon solutions, at monthly temporal resolution, are corrected for the geocentric motion (degree-1) using the Sun et al. (2016) solution. The C_{20} and C_{30} coefficients are derived from Satellite Laser Ranging (SLR) data. The GIA correction for GRACE is based on the ICE6G-D model from (Peltier et al., 2018).

Additionally, the GAD product derived from AOD1B models (Dobslaw et al., 2017; Flechtner et al., 2014), which represents non-tidal atmospheric and oceanic mass redistribution, is added back over the ocean areas to restore the ocean bottom pressure, which combines the effects of ocean mass and atmospheric loading. However, to align GRACE data with altimetry-based sea level (which is corrected for the inverse barometer effect), we convert ocean bottom pressure into manometric ocean mass by subtracting the monthly global ocean-mean atmospheric mass from every grid cell, using the spatial mean of the AOD1B RL06-based GAD product corresponding to each mascon solution (Chen et al., 2019). Note that using the AOD1B RL06 GAD product rather than any updated version is mandatory to maintain strict internal consistency with the background de-aliasing model applied during the RL06 mascon processing.

The CSR, JPL and GSFC products are provided with 0.25°, 0.5° and 0.5° resolution, respectively. They are further interpolated on 1°x1° grids.

Finally, we use the ensemble mean of the three mascon solutions (CSR, JPL, GSFC) as our primary manometric product, deriving structural uncertainties from their ensemble dispersion across the basin (Blazquez et al., 2018; WCRP, 2018).

2.1.3 Argo-based gridded data

The Argo program is an international observational network that deploys a global array of autonomous profiling floats to measure temperature and salinity in the upper 2000m of the ocean. Several institutions process the raw data from these floats and publish gridded temperature (T) and salinity (S) data sets. In this study, we utilize three distinct gridded products: the Scripps Institution of Oceanography (SIO, Roemmich and Gilson, 2009), the Japan Agency for Marine-Earth Science and Technology (JAMSTEC, Hosoda, 2007), and the Met Office Hadley Centre (EN4 product, version 2.2, Cheng et al., 2014). Note that the SIO product rejects salinity profiles exceeding a difference of 0.1 psu when comparing to historical estimate based on the WOCE Global Hydrographic Climatology (Roemmich and Gilson, 2009).

This correction tends to remove the salinity drift reported in Argo floats since 2016 (Liu et al., 2020; Ponte et al., 2021; Wong et al., 2023). The other two products do not apply such a correction. All three data products are available at https://argo.ucsd.edu/data/data-access/ (downloaded in November 2025). The gridded Argo-based time series have a spatial resolution of 1°×1° at monthly interval over January 2004 to December 2022.

2.1.4 Ocean reanalysis

We also used the ocean reanalysis data set CNR-ISMAR Global Historical Reanalysis (CIGAR, Storto and Yang, 2024). CIGAR is a reanalysis system developed by Storto and Yang (2024). Its resolution is 1°x1°. It is based on the NEMO ocean model version 4.0.7 (https://www.nemo-ocean.eu/) and is forced by the ERA5 atmospheric reanalysis from the European Center for Medium-range Weather Forecast (ECMWF) (https://www.ecmwf.int/en/forecasts/dataset/ecmwf-reanalysis-v5). The system uses a three-dimensional variational (3D-Var) scheme to assimilate in situ T/S profiles from the EN4 data set. Notably, CIGAR does not assimilate satellite altimetry data, which allows for independent comparisons. The system consists of 32 ensemble members generated through varying configurations (e.g., perturbed initial conditions and atmospheric forcing). In this study, we use the ensemble mean of the 32 members to derive the thermosteric, halosteric and steric sea level. Bouih et al. (2025) considered the ensemble mean of five ocean reanalyses over 2004-2019, including CIGAR, to compute the manometric component and showed that this ensemble mean and CIGAR manometric components are highly similar. For that reason, here we only consider CIGAR, but extend it until 2022.

Note that, while the CIGAR reanalysis ingests the same T/S measurements as SIO and EN4 (specifically using the EN4 raw in-situ profile dataset), the reanalysis adopts different quality control, observational sub-sampling, mapping (horizontal correlation) methods, and vertical propagation. Additionally, in the reanalysis, other factors connected to the model physics (e.g., vertical mixing) and atmospheric and river forcing further shape the time evolution of the ocean state. The reanalysis thus provides a generally different realization of the ocean state evolution than the other products. Vertical covariances and dynamical processes contribute to the evolution of the deep ocean, unlike observation-only products.

2.2 Methods

2.2.1 Computation of the thermosteric, halosteric and steric components for Argo data and CIGAR reanalysis

The thermosteric, halosteric, and total steric sea level time series are computed from the gridded temperature and salinity products (both reanalyses and gridded observation products) using the Gibbs SeaWater (GSW) Oceanographic Toolbox McDougall et al., 2011), which implements the Thermodynamic Equation Of Seawater (TEOS-10) standard. Specifically, 3D density anomalies are vertically integrated to obtain the total steric sea level; thermo- and halo-steric sea levels are obtained similarly, using density anomalies at constant salinity or temperature, respectively (see https://link.springer.com/article/10.1007/s00382-015-2554-9).

2.2.2 Computation of the manometric component

Manometric sea level change generally refers to the sea-level component associated with ocean mass variations. It is driven by water mass exchange with the continents, such as land ice melt and terrestrial water storage changes, as well as by mass redistribution within the ocean driven by ocean circulation. In this study, because the global mean ocean mass trend is removed, the manometric sea level refers to the regional redistribution of ocean mass around the global mean. In this study, we utilize two methods to obtain an estimate of the manometric component. One method is to use the ensemble mean of the GRACE mascon solutions from CSR, JPL, and GSFC to obtain the GRACE-based manometric estimate. The other method, an alternative to using GRACE solutions, relies on ocean reanalysis data and follows the approach developed by Camargo et al. (2023). Here, we use the sterodynamic sea level provided by the CIGAR ocean reanalysis, which combines steric and dynamic sea level changes. To isolate the manometric component, at every grid mesh, we subtract the local steric value from the sterodynamic variable, both being computed at the same grid mesh. We further add the contemporary Gravitational, Rotational, and Deformation (GRD) fingerprints (representing solid Earth deformations and gravitational effects due to present-day land ice melt and terrestrial water storage changes; Gregory et al., 2019) to obtain a manometric component comparable to GRACE. The sea level fingerprint data used in this study are based on monthly GRD fingerprint grids estimated by Adhikari et al. (2019). Since this original dataset ends in 2016, we extended the time series up to 2022 using linear extrapolation, assuming that the observed trend remains constant after 2016 (see Bouih et al., 2025 for details).

This reanalysis-based estimate is hereafter referred to as CIGAR manometric sea level.

As mentioned above, the CIGAR reanalysis assimilates in-situ T/S profiles. This would mean that the steric and manometric sea levels are not fully independent within the reanalysis due to their dynamical interaction. However, the CIGAR-based manometric component is estimated from the sterodynamic variable that includes both ocean mass redistribution estimated by the model and steric contribution (the latter being further subtracted from the sterodynamic variable). Because the reanalysis is free to adjust the partitioning of sea level variations into steric and manometric components according to the ocean physics and the assimilation framework, without altimetry ingestion, the manometric component constitutes a quasi-independent realization.

2.2.3 Post processing of the data

To ensure spatial consistency across all observing systems, all gridded data sets were spatially interpolated onto a $1° \times 1°$ grid and averaged at monthly interval. Post-processing was performed on such 1°x1° monthly grids. A three-month moving average filter was applied to the corresponding time series. For the spatial analysis, a common mask was applied to all gridded components to exclude regions with high uncertainty. This mask covers latitudes from 66°S to 66°N, excludes inland seas, and omits coastal regions where the distance from land is less than 300 km (see Bouih et al., 2025 for details). For each data set and at each grid mesh, seasonal signals (annual and semi-annual) are removed from the time series through a least-squares adjustment of 6 and 12-month sinusoids, as well as the globally averaged trend of each data set computed over the study period. The study period spans from January 2004 to December 2022. To allow consistent comparison and budget combination across datasets, all gridded anomaly fields and time series were systematically re-referenced to a common baseline period (2004–2009) by subtracting their respective temporal mean over this timeframe.

2.2.4 Data uncertainties

For the altimetry data, we use the uncertainties estimated by Prandi et al. (2021). For the GRACE-based manometric component, uncertainties can be derived from the dispersion of the data sets with respect to the ensemble mean. While formal error estimates are provided with individual mascon solutions (e.g., Watkins et al., 2015), they primarily quantify inversion noise and lack spatial error covariance information, leading to overly optimistic basin-wide uncertainties (< 0.1 mm/yr). Furthermore, as end-users, we have no a priori ground to consider one mascon solution superior to the others. We therefore adopt the ensemble mean of the JPL, CSR, and GSFC solutions as our main manometric dataset. In accordance with established community standards for sea level budget assessments (Barnoud et al., 2021; Blazquez et al., 2018; WCRP, 2018), we estimate the manometric uncertainty from the ensemble dispersion across the three processing centers, which naturally captures the structural processing uncertainty among these equally plausible products.

For the CIGAR-based manometric, thermosteric, halosteric and steric data, the dispersion of the 32 realizations around the ensemble mean was used to estimate the uncertainties.

For the residual time series, the uncertainty was estimated by quadratically summing the error of each term of the budget equation. Regarding the trend uncertainty, it is expressed as the standard error of the least-squares fit. To obtain the uncertainty at the 95% confidence level, we scaled the standard error by a factor of 2 (representing the 2-sigma interval).

3 Results

3.1 Comparison of the different steric products over the North Atlantic

3.1.1 Upper ocean (0-2000m) thermosteric, halosteric and steric products

Figure 1a-d show the thermosteric sea level (TSL) trends over 2004-2022 over the North Atlantic for the three Argo products SIO, JAMSTEC and EN4, and CIGAR (0-2000m) reanalysis data. Similarly, Figure 1e-h shows the halosteric sea level (HSL) trends for the same data sets and period. As expected, due to thermohaline compensation particularly strong in the North Atlantic (e.g., Pardaens et al., 2011; Wang et al., 2010; Wunsch et al., 2007), the two components display opposite trends. Regarding the thermosteric component (Figure 1a-d), all four products display similar spatial patterns, especially indicating significant positive signals in the western North Atlantic. Regarding the halosteric component (Figure 1e-h), the four products share similar spatial patterns; however, the magnitude of the SIO product is slightly smaller than the other three in the Northeast Atlantic, the others being very similar. This difference likely results from the SIO processing that corrects for the instrumental salinity drift reported in Argo floats since 2016, whereas the other products do not account for this. The steric sea level (SSL) trends are shown in Figure 1i-l. The magnitude of the total steric change is smaller than that of the thermosteric component alone. This implies that the halosteric contribution plays a significant compensatory role in the North Atlantic (consistent with previous published studies; e.g., Bouih et al., 2025; Llovel and Hochet, 2025). Unlike in the case of the global mean, the influence of salinity changes on sea level cannot be ignored in this region.

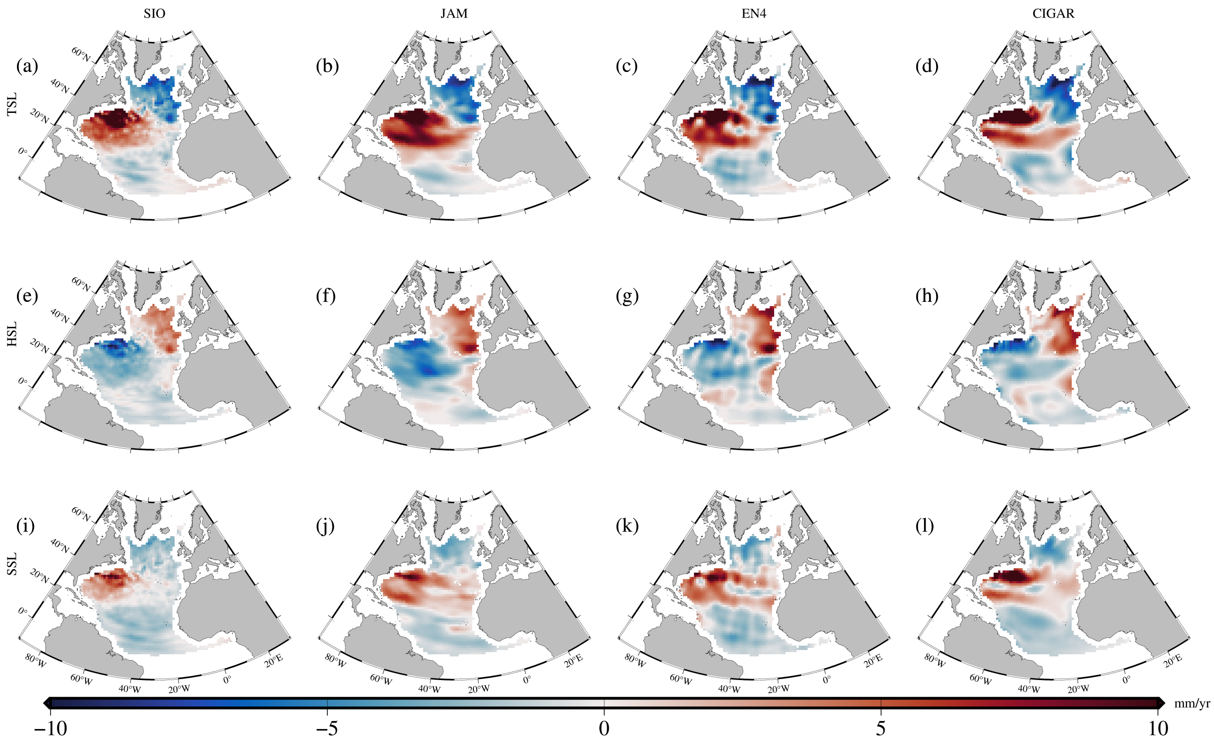

Figure 1. Trends of thermosteric (a–d), halosteric (e–h), and steric (i–l) sea level change in the North Atlantic (0-2000m depth) over 2004–2022 derived from the SIO (a, e, i), JAMSTEC (b, f, j), EN4 (c, g, k) Argo products and CIGAR (d, h ,l) ocean reanalysis.

3.1.2 Full depth thermosteric, halosteric and steric products

Here we use the CIGAR reanalysis data to compute thermosteric, halosteric, and steric sea level changes for the deep ocean (below 2000 m). We consider two cases: (1) SIO upper ocean (0-2000) combined with CIGAR deep ocean (below 2000 m). Hereafter it is called SIO hybrid. (2) CIGAR full depth. Trends of thermosteric, halosteric, and steric full depth for SIO hybrid and CIGAR full depth over 2004–2022 are shown in Figure 2a, c, e for SIO hybrid, and Figure 2b, d, f for CIGAR full depth. Both products display strong positive thermosteric and negative halosteric signals in the western North Atlantic. Small difference is seen for the steric component in the regions of the subtropical gyre between 20°N-40°N, with larger signal near 30°N in the CIGAR full depth case.

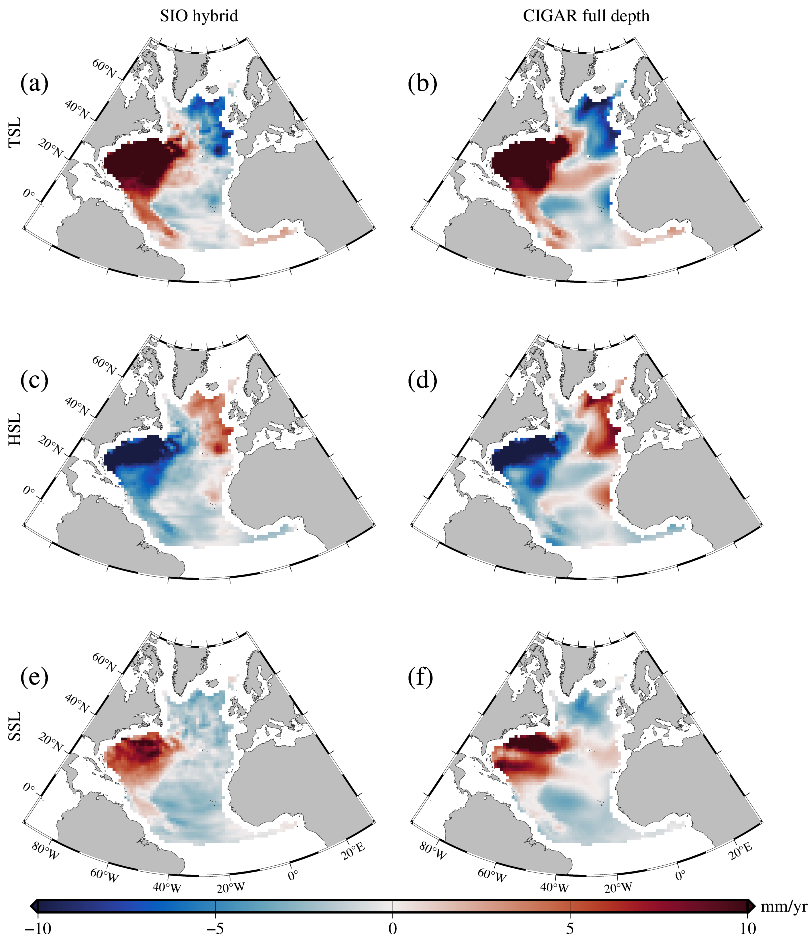

Figure 2. Trends of thermosteric (a, b), halosteric (c, d), and steric (e, f) for SIO hybrid (a, c, e) and CIGAR full depth (b, d, f) sea level change in the North Atlantic over 2004–2022.

3.2 Thermosteric, halosteric and steric time series over 2004-2022 from Argo and CIGAR (0-2000m); (global mean trend removed)

Next, we examine the thermosteric, halosteric and steric time series (weighted averages of the gridded data in the North Atlantic) for the different Argo products and the ocean reanalysis (Figure 3). Figure 3a indicates that the thermosteric component (0-2000m) displays a positive trend in all products as of about 2010. Regarding the halosteric component (0-2000m) (Figure 3b), we observe that the JAMSTEC curve exhibits a spurious positive anomaly between 2008 and 2012. The EN4 curve (and to a little extent the other two datasets) shows a decrease as of 2016, possibly linked to the salinity drift reported in some Argo floats (and not corrected in EN4 and JAMSTEC data), although a potential physical salinity increase cannot be excluded.

The latter issue needs further investigation. In the following, we will only consider the SIO product (as mentioned before, corrected for salinity drift).

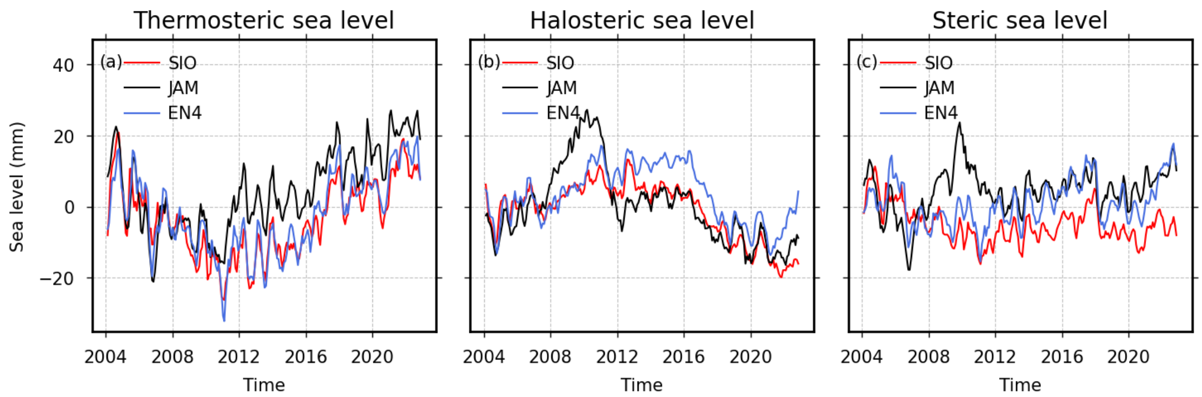

Figure 3. Upper ocean time series of thermosteric (a), halosteric (b), and steric (c) sea level time series in the North Atlantic derived from Argo products (SIO, JAMSTEC, EN4).

3.3 Comparison of the different manometric components over the North Atlantic

Figure 4a, b, shows the manometric spatial trends in the North Atlantic using the GRACE and CIGAR manometric data. The GRACE-based manometric trends for individual mascon solutions are shown in Figure S1 of the Supplementary Information. All three individual solutions show rather similar large-scale patterns, in particular negative manometric trends in the northeast Atlantic.

Comparing Figure 4a and Figure 4b, we distinctly observe contrasting patterns between the GRACE and CIGAR manometric components. For the GRACE-based component, significant negative trends dominate most of the basin, with magnitudes gradually weakening from east to west. Positive trends are however observed in the western tropical Atlantic. In contrast, the CIGAR manometric component displays positive trends in the east and negative trends in the west, separated by a distinct dividing line, which likely corresponds to the position of the Mid-Atlantic Ridge.

Figure 4c,d also shows the 'Altimetry minus steric full depth' trends for both the SIO hybrid and CIGAR cases. These maps are supposed to represent the manometric component. Comparing Figure 4c,d and Figure 4a,b, we note a better agreement between 'Altimetry minus steric full depth' and CIGAR manometric in the eastern Atlantic, both maps showing positive trends, while the GRACE manometric trends are negative in this region. On the other hand, it is worth noting that the positive trend area seen in the GRACE manometric map in the western

Atlantic around 30°N is also seen in the 'Altimetry minus steric full depth' trend map, although with smaller extension, but not in the CIGAR manometric map.

Such comparisons seem point to problems in GRACE data in the eastern North Atlantic region. A recent study by Hightower et al. (2026) revisited the GIA correction applied to GRACE data. They developed a 3D GIA model, considering 3D viscosity fields derived from tomography and two commonly used ice-loading histories. While traditional GIA models assume laterally homogeneous mantle viscosity, these authors show that because the Earth's rheology varies significantly from place to place, it strongly affects how the Earth's mantle rebounds after ice melts, with important impact on the GIA correction applied to GRACE-based ocean mass data in many regions, in particular in the whole Northeast Atlantic. Since here we use GRACE data corrected for the traditional GIA correction, the discrepancy between the GRACE and CIGAR manometric trend maps may result from an inadequate GIA correction.

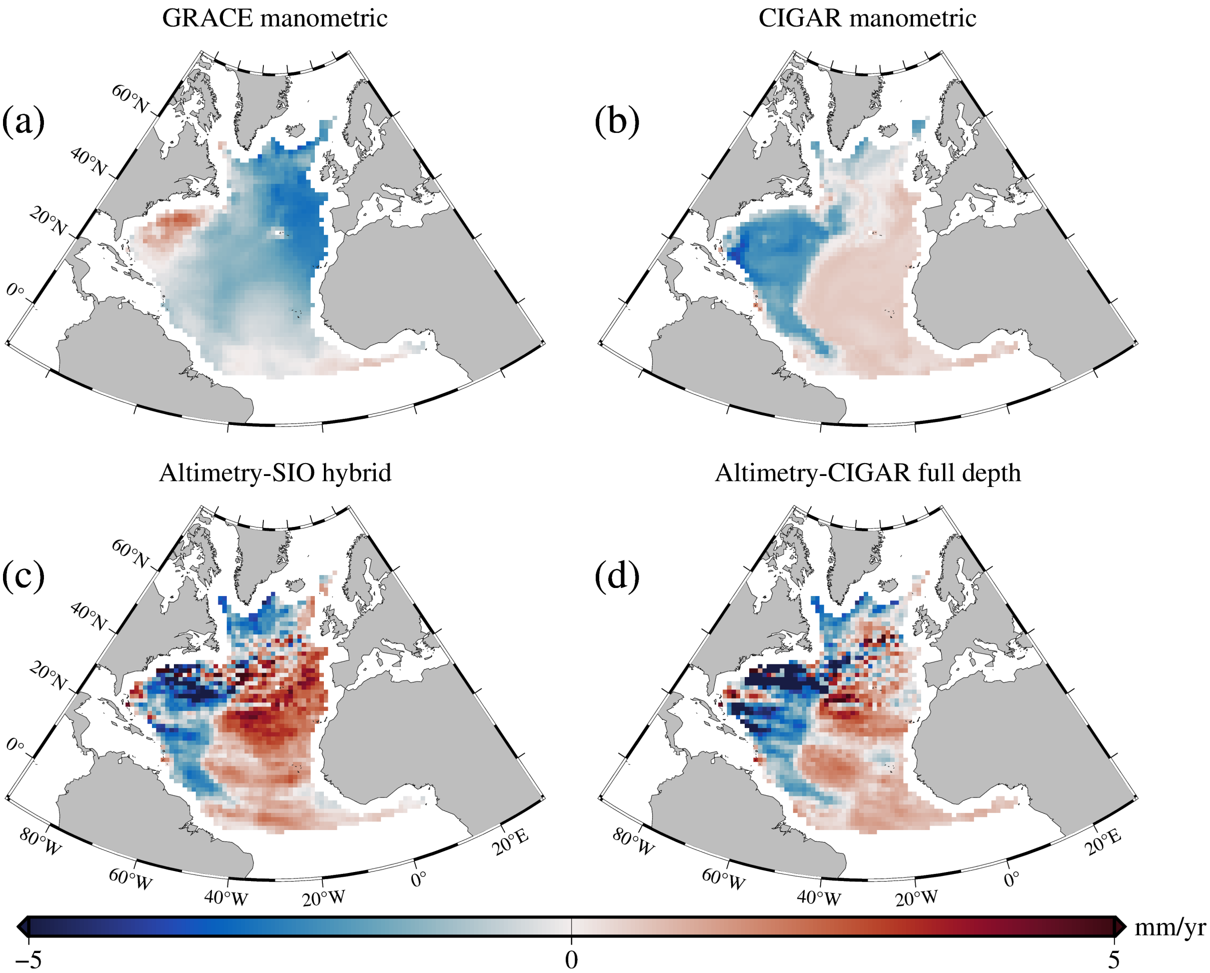

Figure 4. Manometric sea level trends in the North Atlantic over 2004.01-2022.12 derived from (a) the mean of three GRACE mascon solutions, (b) the CIGAR ocean reanalysis, (c) 'Altimetry minus SIO hybrid' and (d) 'Altimetry minus CIGAR full depth'.

3.4 Residual trend maps in the North Atlantic

In this section, we utilize data from the observing systems described above to compute spatial maps of the sea level budget residuals. We compute the residuals by subtracting various combinations of manometric (GRACE, CIGAR) and steric (SIO and CIGAR, upper 2000 m and full depth) components from the altimetry data (Figure 5).

In Figure 5a,b,e,f (upper ocean steric component), the residuals implicitly include the deep ocean steric contribution. As previously observed by Bouih et al. (2025), strong residuals are seen in the Northeast Atlantic with GRACE, and in the Northwest Atlantic with CIGAR. When the deep ocean accounted for (Figure 5c,d,g,h), strong residuals are still seen in the Northeast Atlantic with GRACE, while the residual signal is much attenuated with CIGAR.

Indeed, when using the CIGAR manometric component, the residuals decrease significantly in both spatial variability and magnitude.

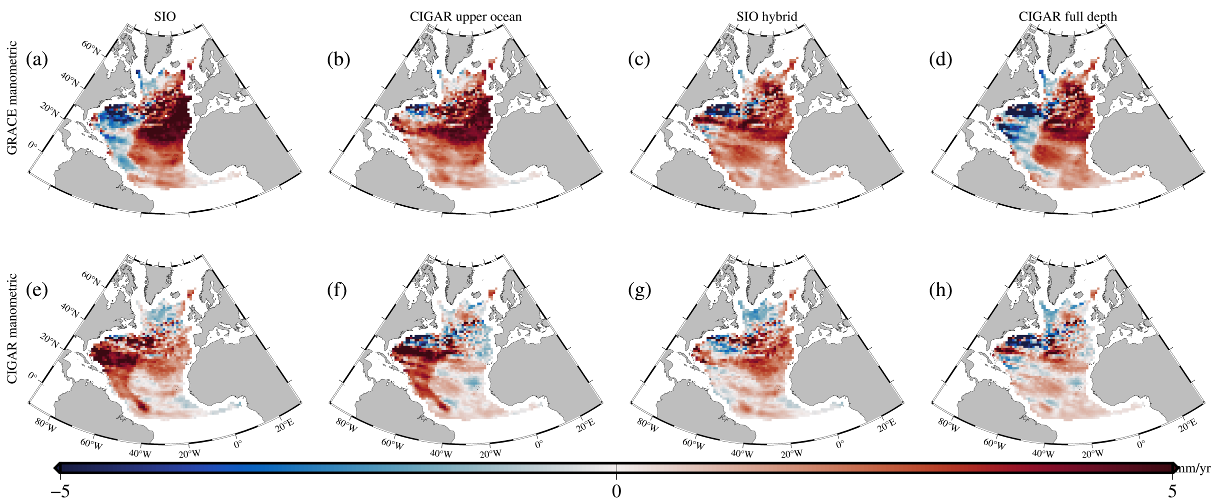

Figure 5. Maps of sea level residuals (mm/yr) in the North Atlantic. The residuals are calculated by subtracting manometric and steric components from satellite altimetry. The manometric component is derived from GRACE (a–d) and CIGAR (e–h). The steric component from SIO (a, e), SIO hybrid CIGAR DO (b, f), CIGAR UP (upper ocean, c, g) and CIGAR full depth (d, h).

To quantify the residual trends, we computed the latitude-weighted spatial mean trend of each map. Results are shown in Table 1. Regardless of the steric data used (whether from SIO or CIGAR), the residuals derived using the CIGAR manometric component are always smaller than those derived using GRACE, for both upper ocean and full depth.

Table 1. Trend values (mm/yr) of sea level residuals in the North Atlantic corresponding to SIO and CIGAR for upper ocean and full depth, and two manometric components. Uncertainties are 2-sigma errors of the least-squares fit (before smoothing).

Trend (mm/yr)	SIO	CIGAR	SIO hybrid	CIGAR full depth
GRACE manometric	2.15±0.19	1.52±0.21	1.53±0.21	0.90±0.23
CIGAR manometric	1.50±0.23	0.86±0.25	0.88±0.25	0.24±0.22

We note that the mean residual magnitude is reduced when the deep-ocean steric change is included: by about 30% when using the GRACE manometric component with SIO upper-2000 m steric sea level, and by about 70% when using the CIGAR manometric component together with the CIGAR full-depth steric component.

3.5 Time series of the North Atlantic mean sea level budget (global mean trends removed)

Figure 6 displays the North Atlantic budget time series using CIGAR for the manometric component and two steric full depth configurations. Figure 6 shows that the CIGAR manometric component display a changing trend as of 2016, which origin remains to be explained. Because of this behavior, the residual curves are not purely linear. However, Figure 6 clearly shows a larger positive trend with SIO hybrid than with CIGAR full depth. Corresponding residual linear trends amount to 0.88±0.20 mm/yr for the SIO hybrid steric case and 0.24±0.22 mm/yr for the CIGAR full-depth case. In the latter case, we may conclude that the North Atlantic sea level budget is closed within data uncertainties.

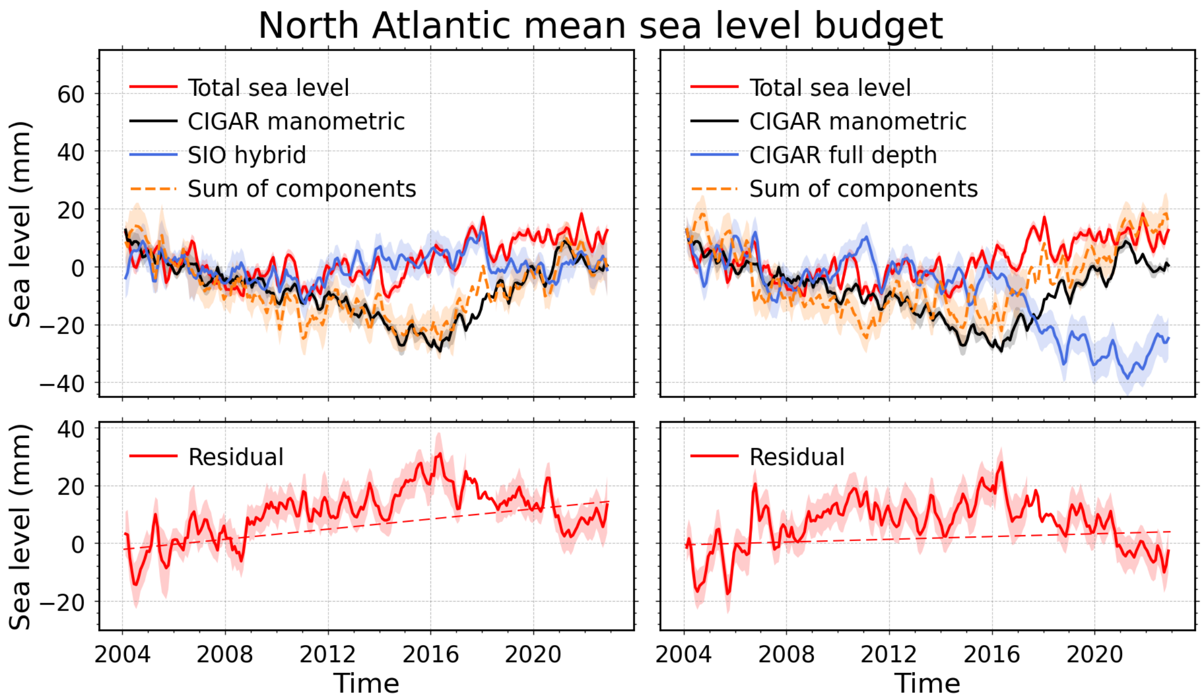

Figure 6. Time series of North Atlantic sea level change components (top) and budget residuals (bottom). The left panels use the SIO hybrid steric estimate, while the right panels use the full-depth CIGAR steric estimate. In both left and right panels, CIGAR manometric components are considered. The global mean trend of each component is removed. Shaded areas represent data uncertainties.

4 Discussion

In this study, we have revisited the sea level budget of the North Atlantic over the 2004-2022 period, using a variety of different data sets. The objective was to further investigate the results from Bouih et al. (2025) who reported non-closure of the sea level budget in the North Atlantic over the same time span, and to identify which components of the budget (or which missing component) are responsible.

The main results of our study can be summarized as follows:

(1) By comparing the GRACE and CIGAR manometric trends with the ‘Altimetry minus steric full depth sea level’, we note a better agreement (same positive sign) between the latter and the CIGAR-based manometric component in the northeastern Atlantic, while the GRACE manometric trends have an opposite (negative) sign in this region. The cause is so far unknown but possibly related to the GIA correction applied to GRACE data, as shown in the recent study by Hightower et al. (2026).

(2) Our study shows that the deep ocean (>2000 m of depth) contribution to the North Atlantic sea level budget is not negligible and needs to be taken into account to obtain better closure of

the sea level budget in this region. Based on CIGAR, the additional deep ocean steric contribution to the North Atlantic sea level budget allows to almost close the regional sea level budget (see Table 1). Accounting for the deep ocean steric contribution reduces by a factor of 30% the residuals of the North Atlantic sea level budget when using the GRACE manometric component, and by a factor of 70% when using CIGAR for the manometric component. In the latter case, the mean residual trend over the North Atlantic is <1mm/yr, i.e., of the same order of magnitude as the regional trend error for altimetry gridded data according to Prandi et al. (2021). We therefore conclude that, almost a small residual remains, the sea level budget closure is achieved within the data uncertainties for this case.

To conclude, these new findings represent a step further towards better understanding of the present-day sea level budget in the North Atlantic region. These investigations also support the need to better observe the deep ocean especially in the North Atlantic Ocean which is one of the objectives of the One Argo Project (Thierry et al., 2025). Nevertheless, some issues still merit deeper investigation. This is particularly the case for the manometric component which shows opposite trends in the Northeast Atlantic when GRACE or CIGAR are considered. Another important issue concerns the exact contribution of the deep ocean. Use of CIGAR (full depth) steric data improves closure of the sea level budget. But whether deep ocean warming still plays a significant role needs to be confirmed using Deep Argo data. Clearly, future studies should be devoted to try answering these remaining questions.

Acknowledgements

The authors thank the editor and the reviewers for helpful comments that significantly improved the manuscript. Zhe Song is supported by China Scholarship Council. This study is a contribution to the ongoing ESA (European Space Agency) CCI (Climate Change Initiative) project entitled ‘Sea level budget closure CCI+ (SLBC_CCI+)’. This work is a contribution to the GREAT project funded by CNES through the Ocean Surface Topography Science Team (OSTST).

Author contributions

AC, WL and ZS designed the study. All analyses have been performed by ZS. ZS and AC wrote a first version of the manuscript. All co-authors contributed to the discussion of the results, editing and final writing of the manuscript.

Competing interests

The contact author has declared that none of the authors has any competing interests.

Data Availability Statement

All data sets used in this study are publicly available and can be accessed from the following sources. The DT2021 gridded altimetry data set is available at Copernicus Climate Change Service, Climate Data Store (2018).

The Argo-based temperature data used to compute the thermosteric time series come from different sources: (a) SIO, data available from https://sio-argo.ucsd.edu/RG_Climatology.html, (b) JAMSTEC, data available from http://www.jamstec.go.jp/ARGO/JARGOe.html., (c) EN4, data available from https://www.metoffice.gov.uk/hadobs/en4/.

The GRACE, GRACE-FO mascon data are available from Save et al. (2016) for CSR (http://www2.csr.utexas.edu/grace), Watkins et al. (2015) for JPL (http://grace.jpl.nasa.gov/) and Loomis et al. (2019) for GSFC (https://earth.gsfc.nasa.gov/geo/data/grace-mascons).

Description of the CIGAR data set, instructions, and data sets are available through the website https://cigar.ismar.cnr.it.

References

Ablain, M., Jugier, R., Zawadzki, L., Taburet, N., Cazenave, A., Meyssignac, B., and Picot, N.: The TOPEX-A drift and impacts on GMSL time series, 2017.

Adhikari, S., Ivins, E. R., Frederikse, T., Landerer, F. W., and Caron, L.: Sea-level fingerprints emergent from GRACE mission data, Earth System Science Data, 11, 629–646, https://doi.org/10.5194/essd-11-629-2019, 2019.

Barnoud, A., Pfeffer, J., Guérou, A., Frery, M., Siméon, M., Cazenave, A., Chen, J., Llovel, W., Thierry, V., Legeais, J., and Ablain, M.: Contributions of Altimetry and Argo to Non-Closure of the Global Mean Sea Level Budget Since 2016, Geophysical Research Letters, 48, https://doi.org/10.1029/2021gl092824, 2021.

Blazquez, A., Meyssignac, B., Lemoine, J., Berthier, E., Ribes, A., and Cazenave, A.: Exploring the uncertainty in GRACE estimates of the mass redistributions at the Earth surface: implications for the global water and sea level budgets, Geophysical Journal International, 215, 415–430, https://doi.org/10.1093/gji/ggy293, 2018.

Bouih, M., Barnoud, A., Yang, C., Storto, A., Blazquez, A., Llovel, W., Fraudeau, R., and Cazenave, A.: Regional sea level trend budget over 2004–2022, Ocean Sci., 21, 1425–1440, https://doi.org/10.5194/os-21-1425-2025, 2025.

Brown, S., Willis, J., and Fournier, S.: Jason-3 Wet Path Delay Correction, https://doi.org/10.5067/J3L2G-PDCOR, 2023.

Camargo, C. M. L., Riva, R. E. M., Hermans, T. H. J., Schütt, E. M., Marcos, M., Hernandez-Carrasco, I., and Slangen, A. B. A.: Regionalizing the sea-level budget with machine learning techniques, Ocean Science, 19, 17–41, https://doi.org/10.5194/os-19-17-2023, 2023.

Chen, J., Tapley, B., Seo, K., Wilson, C., and Ries, J.: Improved Quantification of Global Mean Ocean Mass Change Using GRACE Satellite Gravimetry Measurements, Geophys. Res. Lett., 46, 13984–13991, https://doi.org/10.1029/2019GL085519, 2019.

Chen, J., Tapley, B., Wilson, C., Cazenave, A., Seo, K.-W., and Kim, J.-S.: Global Ocean Mass Change From GRACE and GRACE Follow-On and Altimeter and Argo Measurements, Geophysical Research Letters, 47, e2020GL090656, https://doi.org/10.1029/2020GL090656, 2020.

Cheng, L., Zhu, J., Cowley, R., Boyer, T., and Wijffels, S.: Time, Probe Type, and Temperature Variable Bias Corrections to Historical Expendable Bathythermograph Observations, Journal of Atmospheric and Oceanic Technology, 31, 1793–1825, https://doi.org/10.1175/JTECH-D-13-00197.1, 2014.

Dieng, H. B., Cazenave, A., Meyssignac, B., and Ablain, M.: New estimate of the current rate of sea level rise from a sea level budget approach, Geophysical Research Letters, 44, 3744–3751, https://doi.org/10.1002/2017GL073308, 2017.

Dobslaw, H., Bergmann-Wolf, I., Dill, R., Poropat, L., Thomas, M., Dahle, C., Esselborn, S., König, R., and Flechtner, F.: A new high-resolution model of non-tidal atmosphere and ocean mass variability for de-aliasing of satellite gravity observations: AOD1B RL06, Geophysical Journal International, 211, 263–269, https://doi.org/10.1093/gji/ggx302, 2017.

Flechtner, F., Dobslaw, H., and Fagiolini, E.: GRACE AOD1B product description document for product release 05, 2014.

Frederikse, T., Riva, R., Kleinherenbrink, M., Wada, Y., van den Broeke, M., and Marzeion, B.: Closing the sea level budget on a regional scale: Trends and variability on the Northwestern European continental shelf, Geophysical Research Letters, 43, 10,864-10,872, https://doi.org/10.1002/2016GL070750, 2016.

Gregory, J. M., Griffies, S. M., Hughes, C. W., Lowe, J. A., Church, J. A., Fukimori, I., Gomez, N., Kopp, R. E., Landerer, F., Cozannet, G. L., Ponte, R. M., Stammer, D., Tamisiea, M. E., and van de Wal, R. S. W.: Concepts and Terminology for Sea Level: Mean, Variability and Change, Both Local and Global, Surv Geophys, 40, 1251–1289, https://doi.org/10.1007/s10712-019-09525-z, 2019.

Hamlington, B. D., Gardner, A. S., Ivins, E., Lenaerts, J. T. M., Reager, J. T., Trossman, D. S., Zaron, E. D., Adhikari, S., Arendt, A., Aschwanden, A., Beckley, B. D., Bekaert, D. P. S., Blewitt, G., Caron, L., Chambers, D. P., Chandanpurkar, H. A., Christianson, K., Csatho, B., Cullather, R. I., DeConto, R. M., Fasullo, J. T., Frederikse, T., Freymueller, J. T., Gilford, D. M., Girotto, M., Hammond, W. C., Hock, R., Holschuh, N., Kopp, R. E., Landerer, F., Larour, E., Menemenlis, D., Merrifield, M., Mitrovica, J. X., Nerem, R. S., Nias, I. J., Nieves, V., Nowicki, S., Pangaluru, K., Piecuch, C. G., Ray, R. D., Rounce, D. R., Schlegel, N.-J., Seroussi, H., Shirzaei, M., Sweet, W. V., Velicogna, I., Vinogradova, N., Wahl, T., Wiese, D. N., and Willis, M. J.: Understanding of Contemporary Regional Sea-Level Change and the Implications for the Future, Reviews of Geophysics, 58, e2019RG000672, https://doi.org/10.1029/2019RG000672, 2020.

Horwath, M., Gutknecht, B. D., Cazenave, A., Palanisamy, H. K., Marti, F., Marzeion, B., Paul, F., Le Bris, R., Hogg, A. E., Otosaka, I., Shepherd, A., Döll, P., Cáceres, D., Müller Schmied, H., Johannessen, J. A., Nilsen, J. E. Ø., Raj, R. P., Forsberg, R., Sandberg Sørensen, L., Barletta, V. R., Simonsen, S. B., Knudsen, P., Andersen, O. B., Ranndal, H., Rose, S. K., Merchant, C. J., Macintosh, C. R., von Schuckmann, K., Novotny, K., Groh, A., Restano, M., and Benveniste, J.: Global sea-level budget and ocean-mass budget, with a focus on advanced data products and uncertainty characterisation, Earth System Science Data, 14, 411–447, https://doi.org/10.5194/essd-14-411-2022, 2022.

Hosoda, S.: Grid Point Value of the Monthly Objective Analysis using the Argo data, https://doi.org/10.17596/0000102, 2007.

Liu, C., Liang, X., Chambers, D., and Ponte, R.: Global Patterns of Spatial and Temporal Variability in Salinity from Multiple Gridded Argo Products, Journal of Climate, https://doi.org/10.1175/JCLI-D-20-0053.1, 2020.

Llovel, W. and Hochet, A.: Salinity Contribution to Regional Sea Level Trends in the Tropical Southwestern Pacific Ocean Over 2014–2023, Geophysical Research Letters, 52, e2025GL116115, https://doi.org/10.1029/2025GL116115, 2025.

Llovel, W., Balem, K., Tajouri, S., and Hochet, A.: Cause of Substantial Global Mean Sea Level Rise Over 2014–2016, Geophysical Research Letters, 50, e2023GL104709, https://doi.org/10.1029/2023GL104709, 2023.

Loomis, B. D., Luthcke, S. B., and Sabaka, T. J.: Regularization and error characterization of GRACE mascons, J Geod, 93, 1381–1398, https://doi.org/10.1007/s00190-019-01252-y, 2019.

McDougall, T. J., Barker, P. M., Marine, CSIRO., and Research, A.: Getting started with TEOS-10 and the gibbs seawater (GSW) oceanographic toolbox, Trevor J. McDougall, 2011.

Mu, D., Church, J. A., King, M., Ludwigsen, C. B., and Xu, T.: Contrasting Discrepancy in the Sea Level Budget Between the North and South Atlantic Ocean Since 2016, Earth and Space Science, 11, e2023EA003133, https://doi.org/10.1029/2023EA003133, 2024.

Nerem, R. S., Beckley, B. D., Fasullo, J. T., Hamlington, B. D., Masters, D., and Mitchum, G. T.: Climate-change–driven accelerated sea-level rise detected in the altimeter era, Proceedings of the National Academy of Sciences, 115, 2022–2025, https://doi.org/10.1073/pnas.1717312115, 2018.

Pardaens, A. K., Gregory, J. M., and Lowe, J. A.: A model study of factors influencing projected changes in regional sea level over the twenty-first century, Clim Dyn, 36, 2015–2033, https://doi.org/10.1007/s00382-009-0738-x, 2011.

Peltier, W. R., Argus, D. F., and Drummond, R.: Comment on "An Assessment of the ICE-6G_C (VM5a) Glacial Isostatic Adjustment Model" by Purcell et al.: The ICE-6G_C (VM5a) GIA model, J. Geophys. Res. Solid Earth, 123, 2019–2028, https://doi.org/10.1002/2016JB013844, 2018.

Ponte, R. M., Sun, Q., Liu, C., and Liang, X.: How Salty Is the Global Ocean: Weighing It All or Tasting It a Sip at a Time?, Geophysical Research Letters, 48, e2021GL092935, https://doi.org/10.1029/2021GL092935, 2021.

Prandi, P., Meyssignac, B., Ablain, M., Spada, G., Ribes, A., and Benveniste, J.: Local sea level trends, accelerations and uncertainties over 1993–2019, Sci Data, 8, 1, https://doi.org/10.1038/s41597-020-00786-7, 2021.

Roemmich, D. and Gilson, J.: The 2004–2008 mean and annual cycle of temperature, salinity, and steric height in the global ocean from the Argo Program, Progress in Oceanography, 82, 81–100, https://doi.org/10.1016/j.pocean.2009.03.004, 2009.

Royston, S., Dutt Vishwakarma, B., Westaway, R., Rougier, J., Sha, Z., and Bamber, J.: Can We Resolve the Basin-Scale Sea Level Trend Budget From GRACE Ocean Mass?, Journal of Geophysical Research: Oceans, 125, e2019JC015535, https://doi.org/10.1029/2019JC015535, 2020.

Save, H., Bettadpur, S., and Tapley, B. D.: High-resolution CSR GRACE RL05 mascons: HIGH-RESOLUTION CSR GRACE RL05 MASCONS, J. Geophys. Res. Solid Earth, 121, 7547–7569, https://doi.org/10.1002/2016JB013007, 2016.

Storto, A. and Yang, C.: Acceleration of the ocean warming from 1961 to 2022 unveiled by large-ensemble reanalyses, Nat Commun, 15, 545, https://doi.org/10.1038/s41467-024-44749-7, 2024.

Sun, Y., Riva, R., and Ditmar, P.: Optimizing estimates of annual variations and trends in geocenter motion and J_2 from a combination of GRACE data and geophysical models, J. Geophys. Res. Solid Earth, 121, 8352–8370, https://doi.org/10.1002/2016JB013073, 2016.

Tapley, B., Watkins, M., Flechtner, F., Reigber, C., Bettadpur, S., Rodell, M., Sasgen, I., Famiglietti, J., Landerer, F., Chambers, D., Reager, J., Gardner, A., Save, H., Ivins, E., Swenson, S., Boening, C., Dahle, C., Wiese, D., Dobslaw, H., and Velicogna, I.: Contributions of GRACE to understanding climate change, Nature Climate Change, 5, https://doi.org/10.1038/s41558-019-0456-2, 2019.

Thierry, V., Claustre, H., Pasqueron De Fommervault, O., Zilberman, N., Johnson, K. S., King, B. A., Wijffels, S. E., Bhaskar, U. T. V. S., Balmaseda, M. A., Belbeoch, M., Bollard, M., Boutin, J., Boyd, P., Cancouët, R., Chai, F., Ciavatta, S., Crane, R., Cravatte, S., Dall'Olmo, G., Desbruyères, D., Durack, P. J., Fassbender, A. J., Fennel, K., Fujii, Y., Gasparin, F., González-Santana, A., Gourcuff, C., Gray, A., Hewitt, H. T., Jayne, S. R., Johnson, G. C., Kolodziejczyk, N., Le Boyer, A., Le Traon, P.-Y., Llovel, W., Lozier, M. S., Lyman, J. M., McDonagh, E. L., Martin, A. P., Meyssignac, B., Mogensen, K. S., Morris, T., Oke, P. R., Smith, W. O., Owens, B., Poffa, N., Post, J., Roemmich, D., Rykaczewski, R. R., Sathyendranath, S., Scanderbeg, M., Scheurle, C., Schofield, O., Von Schuckmann, K., Scourse, J., Sprintall, J., Suga, T., Tonani, M., Van Wijk, E., Xing, X., and Zuo, H.: Advancing ocean monitoring and knowledge for societal benefit: the urgency to expand Argo to OneArgo by 2030, Front. Mar. Sci., 12, 1593904, https://doi.org/10.3389/fmars.2025.1593904, 2025.

Wang, C., Dong, S., and Munoz, E.: Seawater density variations in the North Atlantic and the Atlantic meridional overturning circulation, Clim Dyn, 34, 953–968, https://doi.org/10.1007/s00382-009-0560-5, 2010.

Watkins, M. M., Wiese, D. N., Yuan, D.-N., Boening, C., and Landerer, F. W.: Improved methods for observing Earth's time variable mass distribution with GRACE using spherical cap mascons, Journal of Geophysical Research: Solid Earth, 120, 2648–2671, https://doi.org/10.1002/2014JB011547, 2015.

WCRP: Global sea-level budget 1993–present, Earth System Science Data, 10, 1551–1590, https://doi.org/10.5194/essd-10-1551-2018, 2018.

Wong, A. P. S., Gilson, J., and Cabanes, C.: Argo salinity: bias and uncertainty evaluation, Earth System Science Data, 15, 383–393, https://doi.org/10.5194/essd-15-383-2023, 2023.

Wunsch, C., Ponte, R. M., and Heimbach, P.: Decadal Trends in Sea Level Patterns: 1993–2004, Journal of Climate, 20, 5889–5911, https://doi.org/10.1175/2007JCLI1840.1, 2007.